Evaluation Strength of Materials of the Compressor Wheel and Engine Power in the Turbocharger

Tran Huu Danh
Vinh Long University of Technology Education, Vietnam
danhth@vlute.edu.vn

Le Hong Ky
Vinh Long University of Technology Education, Vietnam
kylh@vlute.edu.vn (corresponding author)

Pham Hoang Anh
Vinh Long University of Technology Education, Vietnam
anhph@vlute.edu.vn

Dang Thanh Tam
Vinh Long University of Technology Education, Vietnam
tamdt@vlute.edu.vn

Nguyen Hoang Hiep
Vinh Long University of Technology Education, Vietnam
hiepnh@vlute.edu.vn

Received: 20 May 2024 | Revised: 4 June 2024 | Accepted: 12 June 2024

 DOI: https://doi.org/10.48084/etasr.7891

ABSTRACT

This paper presents the research results on the strength of materials and power of the Toyota 3C engine when changing the structure and number of blades of the compressor wheel in the turbocharger. 3D models of different compressor wheels were created using reverse engineering and then simulated in the ANSYS environment with turbine shaft rotation speeds of 10,000, 15,000, and 20,000 rpm, respectively, to examine the strength of the compression wheel materials. To evaluate engine power, compressor wheels were machined on a 5-axis CNC milling machine. The MP 100S specialized test bed was used to perform experiments and compare engine power when using the original and alternative compressor wheels of the CT9 turbocharger. The compressor wheels were made of aluminum alloy, with a structure and number of blades selected to ensure durability when working. The CT9 turbocharger has a four-pair blade compressor wheel that consistently delivers higher engine power than in other cases.

Keywords-blade structure; compressor wheel; engine power; blade; turbocharger; von-Mises stress

I. INTRODUCTION

A turbocharger is a device operated by the engine's exhaust gas that increases engine efficiency by compressing air into the combustion chambers, making the combustion process more thorough and helping not only save fuel but also reduce emissions that pollute the environment. This device allows more air to be compressed into the engine cylinder, resulting in higher combustion efficiency and increased engine pressure. When heat energy is supplied to a non-turbocharged engine, only 30-40% is converted into useful power, and the physical heat of the external exhaust gas accounts for approximately 40-50%. Using a turbocharger, high-temperature exhaust gases create power before being discharged to drive the turbocharger compressor, increasing the useful power and improving engine fuel consumption. The turbocharger is a device that recovers part of the energy of the exhaust gas, and this recovered energy accounts for 5 to 10% of the total heat energy supplied to the engine [1-3]. Compressor wheels are one of the main turbocharger components and have a very special structure with freely curved surfaces. The design and manufacturing of

turbochargers is a technological secret of manufacturers specializing in automobile and aircraft engines.

Due to the great efficiency that turbochargers bring to different types of engines, research on turbocharger-related content is still a topic of great interest [1-3]. In [4], reverse engineering and rapid prototyping techniques were integrated into the Stereolithography Apparatus (SLA) technique [4] to manufacture turbocharger blades. The SLA technique provides flexibility in design at reduced costs and can be used for visualization and mechanical testing. In [5], the stress on the turbine blades of a turbocharger used in a 118 kW automotive diesel engine was investigated and three different materials and 7-11 blades were examined. The model was created using Solid Works and analyzed in ANSYS 16.0. SolidWorks, Inventor, CATIA software, and others have been used in many design and simulation studies, while ANSYS is used to analyze the von Mises stress structure, displacement, and total deformation of the turbocharger compression wheel [6-8]. Several studies have investigated materials for the manufacture of compression wheels, but aluminum alloy is still the main choice [2-4, 6-8]. There are currently three main methods for machining compressor and turbine wheels: casting, milling on CNC machines, and metal 3D printing. Among them, casting is the classic and most popular manufacturing method [9]. In [4, 10, 11], reverse engineering methods were used to create point cloud files of sample designs, and the machining was programmed in Mastercam software and performed on a 5-axis CNC milling machine. Most previous studies focused only on design and simulation research, with very little mention of compression wheel manufacturing. In addition, most of the studies used reverse engineering methods to design compression wheels. This study inherited these approaches to manufacture compression wheels on a 5-axis CNC milling machine and test engine power on specialized MP 100S equipment.

II. THE COMPRESSOR WHEEL

The turbocharger consists of two main parts: the turbine housing and the compressor housing. The internal structure of the turbocharger includes the turbine wheel, bearings, shaft, compressor wheel, exhaust gas inlets to the inlet manifold and exhaust system, oil supply, oil return, etc. The turbine and compressor wheels are located in separate compartments connected through a central shaft [12]. The turbocharged engine compressor allows more fuel to be loaded, increasing the engine's power. In addition, high intake air pressure improves mixture formation and the combustion process in the engine. In general, turbocharging is an effective measure to increase engine power, allowing improvement of indicators such as reducing the entire engine volume per unit of capacity, reducing the specific weight of the entire engine per unit of power, reducing production costs per unit of power, improving engine efficiency, and reducing harmful emissions [1-3]. This study used a CT9 turbocharger from a Toyota 3C engine with α 2.2 l capacity, a maximum torque/rotation speed of 188-216/1800-2600 Nm/rpm, and a power of 65-67/40000 kW/rpm [13].

A. Turbocharger Compressor Pressure and Velocity

The theoretical basis for the design, simulation, and fabrication of turbocharger compressor wheels is [3]:

- Air enters the compressor at a mean radius with a low velocity V1 and atmospheric pressure P_1.
- Then, its velocity and pressure increase at V_2 and P_2, depending on the centrifugal action of the impeller.
- The air enters the diffuser where its velocity is reduced to V_3 and pressure increases to P_3.

B. Compression Wheel Design

This study investigated the structure and number of blades of the compression wheel. Specifically, instead of the compressor wheel having 4 pairs of blades like the CT9 turbocharger model, as shown in Figure 1(a), this study used 3, 4, and 5 blades, as shown in Figure 2(b-d). The blades had the same shape and surface parameters as the main blade of the sample compression wheel. Reverse engineering was used to design compression wheels as shown in Figure 1 [11, 14]. The structural characteristics (von Mises stress and effective strain) of the compressor wheel sample using aluminum alloy materials were analyzed using ANSYS 2024. The ANSYS Mechanical package was used to define the geometry of the turbine wheel model. The boundary conditions are applied on the compressor wheel, which has a fixed support at the tip of the turbine wheel and the surface of the shaft. Tangential and radial forces are applied to the surface of the blades, and the rotational speed is applied to the surface of the shaft. Figure 2 shows the mesh models with the medium size element. Simulations were performed with turbine shaft rotation speed (and compressor wheel shaft) of 10,000, 15,000, and 20,000 rpm, respectively.

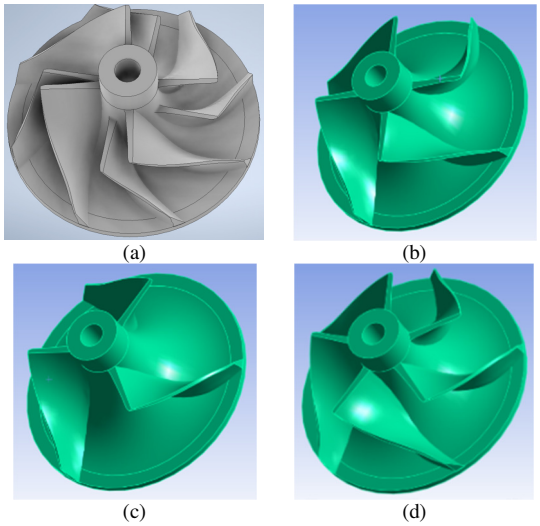

Fig. 1. Model CT9 compression wheel designs.

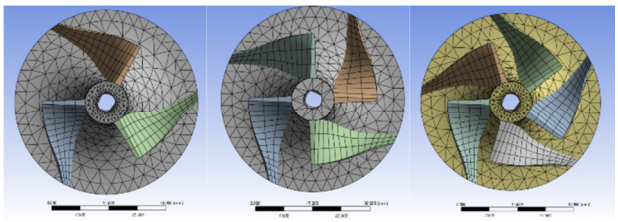

Fig. 2. Mesh models of compressor wheels.

C. Compression Wheel Manufacturing

This study used A6061 aluminum alloy to manufacture the compression wheels, as it has the following characteristics: good corrosion resistance, low melting temperature, tensile strength of 291 MPa, conventional yield strength of 241 MPa, and hardness of 97 HB. Casting is the most popular method for manufacturing turbine and compressor wheels [9]. However, as there are not many parts that need to be machined, this method is costly. This study used a 5-axis Haas CNC milling machine to process the compression wheels, shown in Figures 3 and 4 [10, 15, 16].

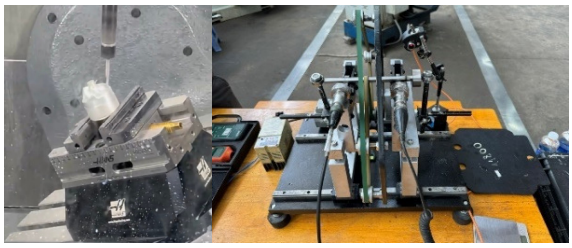

Fig. 3. Compression wheel processing machines and balancing equipment.

Fig. 4. Compressor wheels machined from CNC machines.

III. EXPERIMENTS

A. Experimental Equipment

This study used a Weinlich MP 100S electromagnetic engine power testing device. This device has high accuracy with a wide frequency measurement range and adjustable parameters. This device can be used to measure engine revolutions and engine torque, determine engine power, etc. The device consists of the following main parts: the brake and measuring cluster that is connected to the engine through a propeller shaft and to the control assembly through cables and jacks, the control assembly that includes an internal MP computer and a control panel, a personal computer, a brake controller to change brake force to create load for the engine, and an oscilloscope to display graphs and pulses [17-19].

The machined compressor wheels are dynamically balanced to ensure stable operation with engine speeds up to 2800 rpm and shaft speeds of the compressor wheels in the turbocharger in the range from 10000 rpm to 30000 rpm. Three experiments were carried out for each compressor wheel: standard four-pair-bladed (Bl4-4), single 3-bladed (Bl3), single four-bladed (Bl4), and single 5-bladed (Bl5). The average power value of the motor shaft was obtained as P4-4 (kW), P3 (kW), P4 (kW), and P5 (kW), respectively. The experimental results were stored on the computer using DiaW 1.3.

Fig. 5. Installation of experimental equipment.

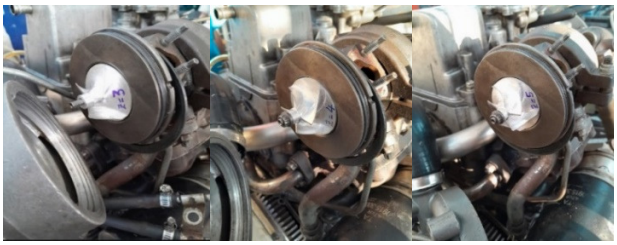

Fig. 6. The installation of compressor wheels in the turbocharger.

B. Engine Capacity Measurement

MP 100S was used to measure the power of the Toyota 3C engine in the following cases: CT9 turbocharger with standard compressor wheel (4 pairs of blades, Bl4-4), fixing the CT9 turbocharger and replacing the compressor wheel with a 3-bladed (Bl3), a four-bladed (Bl4), and a 5-blade (Bl5), respectively. The implementation procedure was as follows:

1. Install the Toyota 3C engine into the MP 100S device.
2. Check the engine fuel, coolant, and lubricating oil.
3. Connect the brake controller to the MP computer of the control assembly.
4. Connect the signal transmission cable from the MP to the personal computer.
5. Turn on the main power switch of the MP 100S device.
6. Calibrate the MP 100S device.
7. Conduct experiments and store results using DiaW 1.3.

IV. RESULTS AND DISCUSSION

A. Simulation Results

Figure 7 shows the von Mises stress simulation results of the 3-blade compressor wheel in different rotation velocities. For a rotational velocity of 10,000 rpm, the maximum von Mises stress was 3.3662 MPa, located on the rear of the compressor blade. For a rotational velocity of 15,000 rpm, the maximum von Mises stress was 4.0057 MPa, located on the rear of the compressor. For a rotational velocity of 20,000 rpm, the maximum von Mises stress was 5.0209 MPa, located on the body of the compressor wheel. Figure 8 shows the simulation results of von Mises stress of the four-blade compressor wheel with different rotation velocities. For a rotational velocity of 10000 rpm, the maximum von Mises stress was 3.3706 MPa, located on the top rear of the compressor blade. For a rotational velocity of 15000 rpm, the maximum von Mises stress was 5.0937 MPa, located on the body of the compressor blade. For a rotational velocity of 20000 rpm, the maximum von Mises stress was 8.0962 MPa, located on the rear of the compressor wheel.Figure 9 shows the simulation results of von Mises stress of the 5-blade compressor wheel in different rotation velocities. For a rotational velocity of 10000 rpm, the maximum von Mises stress was 2.3767 MPa, located on the top rear of the compressor blade. For a rotational velocity of 15000 rpm, the maximum von Mises stress was 3.2049 MPa, located on the top rear of the compressor blade. For a rotational velocity of 20000 rpm, the maximum von Mises stress was 4.2036 MPa, located on the rear of the compressor wheel.

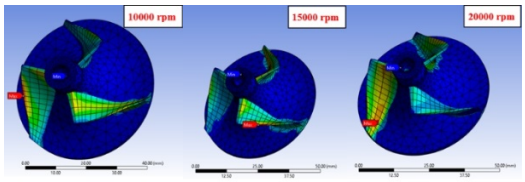

Fig. 7. Simulation results of von Mises stress of a 3-blade compressor wheel with different rotation speeds.

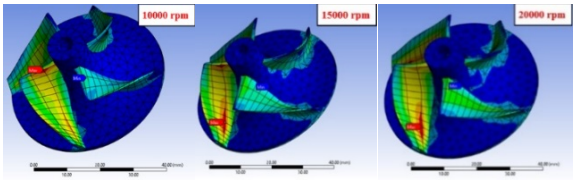

Fig. 8. Simulation results of von Mises stress of a four-blade compressor wheel with different rotation speeds.

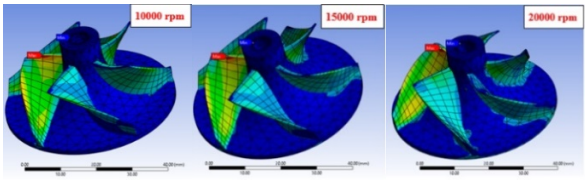

Fig. 9. Simulation results of von Mises stress of a 5-blad compressor wheel with different rotation speeds.

B. Experimental Results

Figure 10 shows torque and power versus the number of revolutions for the original four-pair-bladed compressor wheel. The turbocharger works effectively when the number of revolutions is in the range of 1600 to 2500 rpm. Table I shows the summary of the experimental results with the number of rotation values in the above range [19]. Figure 11 shows the relationship between power and the number of engine revolutions corresponding to the compressor wheels of the turbocharger with different numbers of blades.

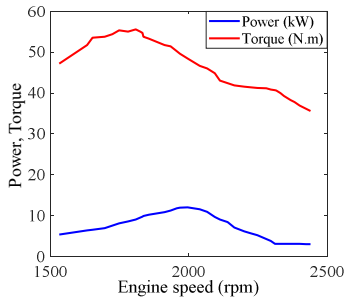

Fig. 10. Relationship between power, torque, and number of engine revolutions.

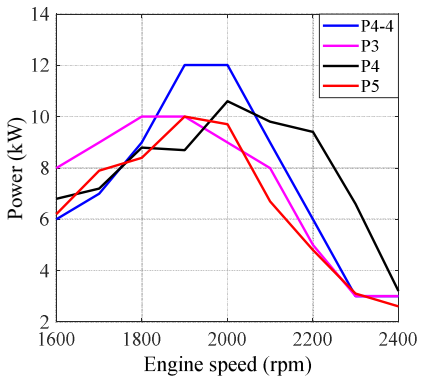

Fig. 11. Relationship between power and number of engine revolutions with different compressor wheels of the CT9 turbocharger.

The average value of engine shaft power corresponding to each compressor wheel of the turbocharger in Table I and Figure 11 shows the following:

- After fully opening the throttle to accelerate the engine, at the time of braking (2400 rpm), the engine power in each measurement is equivalent.
- When controlling the brake counterclockwise to reduce the number of engine revolutions, the engine power tends to increase rapidly, reaching maximum power when the speed is between 1900 and 2000 rpm.
- When controlling the brake to reduce the engine speed to 1000 rpm, the engine power tends to decrease.
- The turbocharger with a four single-bladed compressor wheel (Bl4) produces engine power that is always higher than the other cases when working at speeds above 2000 rpm.

TABLE I. ENGINE POWER MEASUREMENT RESULTS

No	n (rpm)	P4-4 (kW)	P3 (kW)	P4 (kW)	P5 (kW)
1	1600	6	8	6.8	6.2
2	1700	7	9	7.2	7.9
3	1800	9	10	8.8	8.4
4	1900	12	10	8.7	10
5	2000	12	9	10.6	9.7
6	2100	9	8	9.8	6.7
7	2200	6	5	9.4	4.8
8	2300	3	3	6.6	3.1
9	2400	3	3	3.2	2.6

In general, engine power is lower when the turbocharger compressor wheel is only single-bladed compared to the case of using the original compressor wheel (4 pairs of blades). Exceptionally, the turbocharger with compressor wheel Bl4 working at a speed above 2060 rpm and Bl3 working at a speed below 1840 rpm has higher engine power compared to the case of using the sample compressor wheel. The summary of von Mises equivalent stress analysis and experimental results show that the compressor wheel with 4 single blades (Bl4) provides high engine power but lower strength of material parts when working at high speed.

V. CONCLUSION

Simulation results showed that with compressor wheels having three and five single blades, the maximum von Mises equivalent stress corresponding to different rotation speeds is below 5.0210 Mpa. In the case of a compressor wheel with four blades, when the rotation speed is 15,000 rpm, the maximum von Mises stress is 5.0937 MPa, located on the blade body of the compressor wheel. When the rotation speed is 20000 rpm, the maximum von Mises stress is up to 8.0962 MPa, located behind the compressor wheel. The MP 100S specialized test bed was used to carry out experiments comparing engine power when using the designed compressor wheels with the standard compressor wheel of the CT9 turbocharger. Experimental results showed that, in general, the engine power is lower when the turbocharger compressor wheels are single-bladed compared to when using the standard four-pair-blade compressor wheel. However, there is an exception with turbochargers with four (Bl4) and three (Bl3) single-bladed compressor wheels, as they worked better at speeds above 2060 rpm and below 1840 rpm, respectively, as their dynamic power does not follow the general trend. In addition, at speeds above 2000 rpm, the turbocharger with the Bl4 compressor wheel produced engine power that was always higher than the other designs.

REFERENCES

[1] K. Hazizi, "Aerodynamic Optimisation of Turbocharger Compressor Diffuser Geometry for Real-World Drive Cycles," Ph.D. dissertation, Anglia Ruskin University, Cambridge, UK, 2021.

[2] S. K. Bohidar, P. K. Sen, and R. Bharadwaj, "Study of Turbo Charging," *International Journal of Advanced Technology in Engineering and Science*, vol. 3, no. 1, pp. 498–505, Apr. 2015.

[3] S. Thorat, "Centrifugal Compressor - Diagam, Parts, Working, Efficiency, Advantages." Hydraulic and Pneumatic System, Learn Mechanical Engineering. https://learnmech.com/centrifugal-compressor-diagram-parts-working-advantages.

[4] B. Mallikarjuna and Dr. U. Chandrashekar, "Innovative Modeling and Rapid Prototyping of Turbocharger Impeller," *Science and Engineering of Composite Materials*, vol. 2, no. 9, pp. 1426–1432, Sep. 2013.

[5] A. A. Thet, A. K. Latt, S. Y. Htwe, and M. Zaw, "Analysis of Turbine Blade for Automobile Turbocharger by Changing Material and Number of Blades," *Iconic Research And Engineering Journals (IRE Journals)*, vol. 2, no. 6, pp. 122–127, 2018.

[6] N. N. Hlaing, H. H. Win, M. Thein, and A. K. Latt, "Structural Analysis of Compressor Blades for Turbocharger by Using the Different Materials," *International Journal of Advances in Scientific Research and Engineering (Ijasre)*, vol. 5, no. 12, pp. 94–104, Dec. 2019, https://doi.org/10.31695/IJASRE.2019.33643.

[7] N. Sathishkumar, P. Premkumar, A. R. Bruce, K. Pravinkumar, and P. L. Sudharsan, "Design and Analysis of an Impeller of a Turbocharger," *International Journal of Research and Review*, vol. 7, no. 4, pp. 45–51, Apr. 2020, https://doi.org/10.4444/ijrr.1002/1871.

[8] D. R. Kumar, B. Shanmugasundaram, and P. Mohanraj, "Design and Analysis of Turbocharger Impeller in Diesel Engine," *International Journal of Advance Mechanical and Mechanics Engineering*, vol. 1, no. 1, pp. 1–15, 2017.

[9] T. Sotome and S. Sakoda, "Development of Manufacturing Technology for Precision Compressor Wheel Castings for Turbochargers," *Furukawa Review*, vol. 32, pp. 56–60, 2007.

[10] H. K. Le, "A Study on the Influence of Plasma Nitriding Technology Parameters on the Working Surface Deformation of Hypoid Gears," *Engineering, Technology & Applied Science Research*, vol. 12, no. 6, pp. 9760–9765, Dec. 2022, https://doi.org/10.48084/etasr.5365.

[11] L. H. Ky and T. V. Hung, "The Effects of Technological Parameters on the Accuracy and Surface Roughness of Turbine Blades When Machining on CNC Milling Machines," in *Proceedings of the International Conference on Advanced Mechanical Engineering, Automation, and Sustainable Development 2021 (AMAS2021)*, Ha Long, Vietnam, Nov. 2021, pp. 276–284, https://doi.org/10.1007/978-3-030-99666-6_42.

[12] M. Moorthi, "Turbocharger." Linkedin. https://www.linkedin.com/pulse/turbocharger-moorthi-m-23pqc.

[13] "NEW CT9 17201-64070 Turbo Turbocharger for TOYOTA Estima Emina Lucida,3C-T 2.2L 90HP." https://vi.aliexpress.com/item/547984662.html.

[14] C. N. Van, A. L. Hoang, C. D. Long, and D. N. Hoang, "Surface Roughness in Metal Material Extrusion 3D Printing: The Influence of Printing Orientation and the Development of a Predictive Model," *Engineering, Technology & Applied Science Research*, vol. 13, no. 5, pp. 11672–11676, Oct. 2023, https://doi.org/10.48084/etasr.6162.

[15] N. H. Hiep, L. H. Ky, P. H. Anh, L. H. K. Duyen, and T. V. Hung, "An Evaluation of Some Specifications of Turbine Blades Made by 3D Printing Technology and Processed on CNC Milling Machines," in *Advances in Engineering Research and Application (ICERA 2022)*, Thai Nguyen, Vietnam, Dec. 2022, pp. 177–187, https://doi.org/10.1007/978-3-031-22200-9_19.

[16] N. T. Van and L. H. Ky, "The Influence of Plasma Nitriding Technology Parameters on the Hardness of 18ХГТ Steel Parts," *Engineering, Technology & Applied Science Research*, vol. 14, no. 2, pp. 13643–13647, Apr. 2024, https://doi.org/10.48084/etasr.7089.

[17] *MP 100 S engine test bed with MP computer operating instructions*. Weinlich Steuerungen, Reilingen, Germany.

[18] D. D. Trung, "Multi-objective optimization of SKD11 Steel Milling Process by Reference Ideal Method," *International Journal of Geology*, vol. 15, pp. 1–16, Apr. 2021, https://doi.org/10.46300/9105.2021.15.1.

[19] D. D. Trung, "Multi-criteria decision making of turning operation based on PEG, PSI and CURLI methods," *Manufacturing Review*, vol. 9, Apr. 2022, Art. no. 9, https://doi.org/10.1051/mfreview/2022007.